Hindawi Publishing Corporation
Advances in Condensed Matter Physics
Volume 2013, Article ID 136274, 7 pages
http://dx.doi.org/10.1155/2013/136274

Research Article

Structural, Elastic, and Electronic Properties of Antiperovskite Chromium-Based Carbides $ACCr_3$ (A = Al and Ga)

D. F. Shao,[1] W. J. Lu,[1] S. Lin,[1] P. Tong,[1] and Y. P. Sun[1,2]

[1] *Key Laboratory of Materials Physics, Institute of Solid State Physics, Chinese Academy of Sciences, Hefei 230031, China*
[2] *High Magnetic Field Laboratory, Chinese Academy of Sciences, Hefei 230031, China*

Correspondence should be addressed to W. J. Lu; wjlu@issp.ac.cn and Y. P. Sun; ypsun@issp.ac.cn

Received 29 October 2012; Accepted 24 December 2012

Academic Editor: Laifeng Li

We theoretically investigated antiperovskite chromium-based carbides $ACCr_3$ through the first-principles calculation based on density functional theory (DFT). The structure optimization shows that the lattice parameter of $ACCr_3$ is basically proportional to the radius of A-site elements. The calculated formation energies show that $AlCCr_3$ and $GaCCr_3$ can be synthesized at ambient pressure and are stable with nonmagnetic ground states. Based on the calculation of elastic constants, some elastic, mechanical, and thermal parameters are derived and discussed. $AlCCr_3$ and $GaCCr_3$ show ductile natures and may have similar thermal properties. From the analysis of the electronic structures, it was found that there are electron and hole bands that cross the Fermi level for $AlCCr_3$ and $GaCCr_3$, indicating multiple-band natures. The Fermi level locates at the vicinity of the density of states (DOSs) peak, which leads to a large DOS at Fermi level dominated by Cr-3d electrons. The band structures of $AlCCr_3$ and $GaCCr_3$ are very similar to those of the superconducting antiperovskite $MgCNi_3$. The similarity may make $AlCCr_3$ and $GaCCr_3$ behave superconductively, which needs to be further investigated in theoretical and experimental studies.

1. Introduction

Recently, antiperovskite compounds AXM_3 (A, main group elements; X, carbon, boron, or nitrogen; M, transition metal) have attracted considerable attention. Due to the high concentration of transition metals in a cell, it can be deduced that interesting properties will be found in the family of compounds. In the antiperovskites family, nickel-based and manganese-based antiperovskites were extensively studied. Abundant physical properties were shown in the two kinds of compounds, such as superconductivity [1–3], giant magnetoresistance (MR) [4, 5], large negative magnetocaloric effect (MCE) [6, 7], giant negative thermal expansion [8, 9], magnetostriction [10], and nearly zero temperature coefficient of resistivity [11, 12]. But there are only a few reports about other 3d-metal-based antiperovskites so far. The difficulty restricting researchers is the exploration of new materials that can be experimentally synthesized. Therefore, theoretical investigations on these potential 3d-metal-based antiperovskites are useful to find the easily prepared stable materials and explore the new physical properties.

In the earlier years, researchers have found that in chromium compounds there are varieties of interesting physical properties. Many of chromium alloys such as Cr-Ru, Cr-Rh, and Cr-Ir alloys show superconductivity [13]. And it was found there is spin density wave antiferromagnetism that coexists with superconductivity in $Cr_{1-x}Re_x$ ($x > 0.17$) [14], $Cr_{1-x}Ru_x$ ($x > 0.17$) [15], and $(Cr_{1-x}Mo_x)_{75}Ru_{75}$ ($x = 0$, 0.03, 0.06, and 0.10) [16]. For chromium-based antiperovskites, Wiendlocha et al. [17] discussed the possibility of superconductivity in $GaNCr_3$ and $RhNCr_3$, and recent phonon and electron-phonon coupling calculation of $RhNCr_3$ [18] supports Wiendlocha et al.'s prediction. In the present work, we theoretically investigated antiperovskite chromium-based carbides $ACCr_3$ through the first-principles calculation based on density functional theory (DFT). The optimized lattice parameter of $ACCr_3$ is basically proportional to the radius of A-site elements. From the analysis of formation energies, we predict that only $AlCCr_3$ and $GaCCr_3$ can be synthesized at ambient pressure, and they are stable with nonmagnetic ground states. The elastic and electronic properties of the two compounds are specifically discussed.

Table 1: The coefficient A_2 in (1) as combinations for second order elastic constant for cubic crystal. η_α denotes the Lagrangian strain tensors in terms of ξ.

Strain type	A_2
$\eta_1 = (\xi, 0, 0, 0, 0, 0)$	C_{11}
$\eta_2 = (\xi, \xi, 0, 0, 0, 0)$	$2C_{11} + 2C_{12}$
$\eta_3 = (\xi, \xi, \xi, 0, 0, 0)$	$C_{11} + 4C_{44}$

$AlCCr_3$ and $GaCCr_3$ show ductile natures and may have similar thermal properties. The electron and hole bands cross the Fermi level, implying the multiple-band nature of $AlCCr_3$ and $GaCCr_3$. The Fermi level locates at the vicinity of the density of states (DOS) peak, which leads to a large DOS at Fermi level dominated by Cr-3d electrons. The bands properties of $AlCCr_3$ and $GaCCr_3$ are very similar to those of superconducting antiperovskite $MgCNi_3$. The similarity may make $AlCCr_3$ and $GaCCr_3$ show superconductivity.

2. Computational Details

The calculations were performed by projected augmented-wave (PAW) [19, 20] method using the ABINIT code [21–23]. The PAW method can lead to very accurate results comparable to other all-electron methods. For the exchange-correlation functional, the generalized gradient approximation (GGA) according to the Perdew-Burke-Ernzerhof [24] parametrization was used. Electronic wavefunctions are expanded with plane waves up to an energy cutoff of 1200 eV. Brillouin zone sampling is performed on the Monkhorst-Pack (MP) mesh [25] of 16 × 16 × 16. The self-consistent calculations were considered to be converged when the total energy of the system was stable within 10^{-6} Ha. Nonmagnetic, ferromagnetic (FM), and antiferromagnetic (AFM) states were tested in the study. For AFM states, we only considered the simplest case: the spins of Cr atom in [111] layers are parallel with each other in the same layer and are antiparallel with spins in the neighboring layers.

The elastic constants are evaluated according to the finite-strain continuum elasticity theory [26, 27]. The strain energy per unit mass can be expressed as a polynomial of the strain parameter ξ [28]:

$$\phi(\xi) = \frac{1}{2}A_2\xi^2 + \frac{1}{6}A_3\xi^3 + O\left(\xi^4\right), \tag{1}$$

where the coefficients A_2 and A_3 are combinations of second- and third-order elastic constants of the crystal, respectively. For a cubic structure, there are three independent second-order elastic constants (C_{11}, C_{12}, and C_{44}). Therefore, here we introduced 3 Lagrangian strain tensors labeled as η_α in terms of ξ. η_α and the corresponding coefficients A_2 are listed in Table 1.

Once the single-crystal elastic constants are calculated, the related elastic and mechanic parameters may also be evaluated. Using the Voigt-Reuss-Hill approximation [29], bulk modulus B and shear modulus G of cubic crystal can be defined as

$$B = \frac{C_{11} + 2C_{12}}{3}, \tag{2}$$

$$G = \frac{G_V + G_R}{2}, \tag{3}$$

where the subscripts V and R denote the Voigt, and Reuss average, respectively. In (3),

$$G_V = \frac{C_{11} - C_{12} + 3C_{44}}{5}, \qquad G_R = \frac{5\left(C_{11} - C_{12}\right)C_{44}}{4C_{44} + 3\left(C_{11} - C_{12}\right)}. \tag{4}$$

Thus Young's modulus E and Poisson's ratio σ can be obtained using the relations

$$E = \frac{9BG}{3B + G}, \qquad \sigma = \frac{3B - 2G}{2\left(3B + G\right)}. \tag{5}$$

Using the calculated bulk modulus B, shear modulus G, and Young's modulus E, the Debye temperature Θ_D can be determined as

$$\Theta_D = \frac{h}{k_B}\left(\frac{3n\rho N_A}{4\pi M}\right)^{1/3} \upsilon_m, \tag{6}$$

where h, k_B, and N_A are Planck's, Boltzmann's constants, and Avogadro's number, respectively. ρ is the mass density, M is the molecular weight, and n is the number of atoms in the unit cell. The mean sound velocity is defined as

$$\upsilon_m = \left[\frac{1}{3}\left(\frac{2}{\upsilon_t^3} + \frac{1}{\upsilon_l^3}\right)\right]^{1/3}, \tag{7}$$

where υ_l and υ_t are the longitudinal and transverse sound velocities, which can be obtained from bulk modulus B and shear modulus G:

$$\upsilon_l = \left(\frac{3B + 4G}{3\rho}\right)^{1/2}, \qquad \upsilon_t = \left(\frac{G}{\rho}\right)^{1/2}. \tag{8}$$

3. Results and Discussion

3.1. Ground State and Formation Energy. The structures were fully optimized with respect to lattice parameter and atomic positions. The optimized lattice parameters of $ACCr_3$ for different A-site elements are listed in Table 2. The results show that the lattice parameter of $ACCr_3$ is basically proportional to the radius of A-site elements (see Figure 1).

The common technique for producing antiperovskite carbides is the solid-state synthesis from the parent materials.

Table 2: Lattice parameter a, magnetic moments per Cr atom M, and the formation energies ΔE of $ACCr_3$.

	a (Å)	ΔE_{NM} (eV/atom)	ΔE_{FM} (eV/atom)	M_{FM} (μ_B/Cr)	ΔE_{AFM} (eV/atom)	M_{AFM} (μ_B/Cr)
$CuCCr_3$	3.869	0.214	0.212	0.396	0.205	1.006
$ZnCCr_3$	3.894	0.125	0.126	0.127	0.115	1.020
$GaCCr_3$	3.891	−0.019	−0.019	0.001	−0.019	0.099
$MoCCr_3$	3.898	0.105	0.105	0.053	0.105	0.240
$AlCCr_3$	3.887	−0.0479	−0.0478	0.034	−0.0478	0.212
$AgCCr_3$	3.936	0.286	0.292	0.544	0.268	1.649
$CdCCr_3$	3.973	0.256	0.257	0.341	0.213	2.102
$SnCCr_3$	3.981	0.082	0.0786	0.400	0.082	0.000
$MgCCr_3$	3.952	0.220	0.219	0.173	0.195	1.824
$InCCr_3$	3.999	0.187	0.189	0.406	0.188	0.006
$YCCr_3$	4.088	0.269	0.268	0.611	0.270	0.000
$LaCCr_3$	4.122	0.496	0.362	1.8101	0.497	0.002
$CaCCr_3$	4.083	0.539	0.541	0.3311	0.539	0.001
$SrCCr_3$	4.155	0.795	0.795	0.402	0.796	0.002
$BaCCr_3$	4.246	1.166	0.998	1.957	1.166	0.002

Table 3: Elastic constants and derived quantities for $ACCr_3$ (A = Al and Ga).

	C_{11} (GPa)	C_{12} (GPa)	C_{44} (GPa)	A	C_p (GPa)	B (GPa)	G (GPa)	B/G	E (GPa)	σ	Θ_D (K)
$AlCCr_3$	448.18	297.98	68.31	0.91	229.67	348.04	70.95	4.90	199.30	0.40	532.43
$GaCCr_3$	480.81	314.43	64.63	0.78	249.80	369.89	71.51	4.40	201.53	0.41	497.12

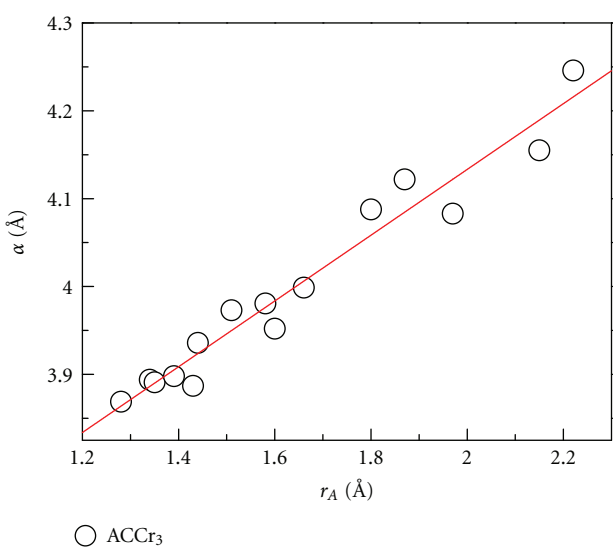

Figure 1: Relation between the lattice parameter a and the radius of A-site elements r_A.

Therefore we assumed that the antiperovskite chromium-based carbides $ACCr_3$ could be synthesized in the same routine. We analyze the stability of compounds by calculating the formation energies ΔE, which is defined as the difference between the total energies of initial reagents (elements) and final compounds:

$$\Delta E = E_{tot}^{ACCr_3} - \left(E_{tot}^{A} + E_{tot}^{C} + 3E_{tot}^{Cr}\right). \quad (9)$$

Here, E_{tot}^{A}, E_{tot}^{C}, and E_{tot}^{Cr} are the total energies of the initial reagents.

According to the definition of ΔE, negative values indicate that the formation of compounds from the initial components is energetically favorable and the compounds are stable with respect to a mixture of the initial elements. Conversely, if $\Delta E > 0$, the compounds are unlikely to be synthesized under normal conditions.

The calculated ΔE for the series of A-site elements with different magnetic configurations are listed in Table 2. Except for $AlCCr_3$ and $GaCCr_3$, all other compounds show positive ΔE. For $AlCCr_3$ and $GaCCr_3$, the values of ΔE for different magnetic configurations are very close, and the magnetic moments per Cr atom for the FM and AFM states are very small, which implies the nonmagnetic ground states of $AlCCr_3$ and $GaCCr_3$. From the analysis of formation energies, it seems that $ACCr_3$ can be synthesized only when A = Al and Ga. The elastic and electronic properties of the two compounds will be discussed later.

3.2. Elastic and Mechanical Properties. In order to obtain accurate elastic constants, ξ is varied with a step of 0.0025 in every case for η_α. As an example, the strain energies for $AlCCr_3$ and the fitted polynomials are shown in Figure 2. The calculated elastic constants at ambient pressure and other derived mechanical parameters are listed in Table 3. From the calculated values of the elastic constants, one can find that they satisfy the mechanical stability criteria for a cubic crystal, that is, $C_{11} > C_{12}$, $C_{44} > 0$, and $C_{11} + 2C_{12} > 0$ [30], which indicates that the compounds are mechanically stable.

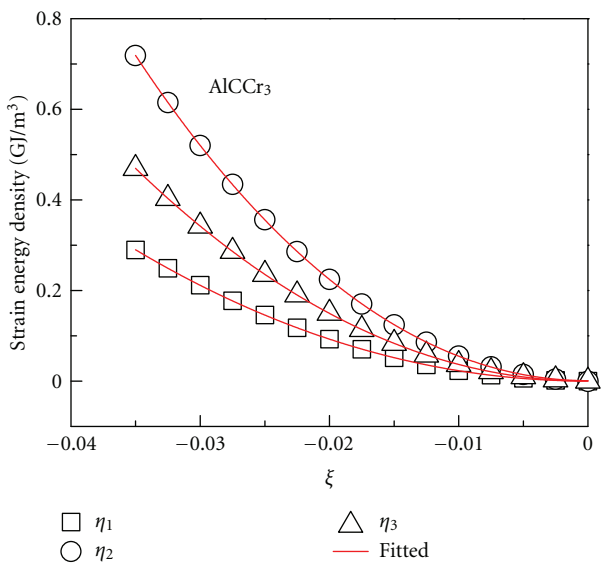

Figure 2: The strain-energy relation of $AlCCr_3$.

Cracks in crystals are directly related to the anisotropy of thermal and elastic properties [31]. The elastic anisotropy factor A of cubic crystal can be described as

$$A = \frac{2C_{44}}{C_{11} - C_{12}}. \tag{10}$$

For a complete isotropic system, the anisotropy factor A takes the value of unity, and the deviation from unity measures the degree of elastic anisotropy [32]. The elastic constant C_{44} represents the shear resistance in a [100] direction, which is related to the C–Cr bonding. The values of C_{44} for the two compounds are almost the same, which implies the similar C–Cr bonding nature of the two compounds. $C_{11} - C_{12}$ turns out to be the stiffness associated with a shear in a [110] direction, which can be connected with the bonding between A–Cr bonding. Although A–M bonding is usually very weak in antiperovskite ACM_3, it still can influence the anisotropy of the material. The anisotropic factors A are listed in Table 3. The different A–Cr bondings of the two compounds lead to different anisotropy. For $AlCCr_3$, $A = 0.91$ indicates that $AlCCr_3$ is almost isotropic. However, $GaCCr_3$ seems like more anisotropic ($A = 0.78$).

Young's modulus E defines the ratio between the linear stress and strain. The larger the value of E, the stiffer is the material. In general, as Young's modulus increases, the covalent nature of the compound also increases, which further has an impact on the ductility of the compounds. The values of E for $AlCCr_3$ and $GaCCr_3$ are very close to each other, suggesting the similar covalent nature of the two compounds.

The Cauchy's pressure C_p is defined as the difference between the two particular elastic constants $C_p = C_{12} - C_{44}$. It is considered to serve as an indication of ductility: $C_p > 0$ suggests that the material is expected to be ductile; otherwise, the material is expected to be brittle [33]. As shown in Table 3, the values of C_p for $AlCCr_3$ and $GaCCr_3$ are positive, which is a clear indication for the compounds to be ductile. Another index of ductility is the ratio B/G. According to Pugh [34], the ductile/brittle properties of materials could be related empirically to the ratio B/G. If $B/G > 1.75$, the material would be ductile; otherwise the material behaves in a brittle manner. For $ACCr_3$ (A = Al and Ga), all the calculated B/G ratios are much larger than 1.75, which clearly highlights the ductile nature of $ACCr_3$ (A = Al and Ga). Poisson's ratio generally quantifies the stability of the crystal against shear and takes the value between −1 and 0.5, which are the lower and the upper bounds. The lower bound is where the material does not change its shape, and the upper bound is where the volume remains unchanged. The calculated σ of $ACCr_3$ (A = Al and Ga), listed in Table 3, are very close to the typical σ value of 0.33 for ductile metallic materials [35]. All the parameters clearly show the ductility of $ACCr_3$ (A = Al and Ga).

Using bulk modulus B, shear modulus G, and Young's modulus E, the Debye temperature Θ_D can be calculated. As a matter of fact, a higher Θ_D would imply a higher thermal conductivity associated with the material [36]. For the present calculation, the Θ_D are estimated to be 532.43 K and 497.12 K for $AlCCr_3$ and $GaCCr_3$, respectively. The similar values of Θ_D suggest the similar thermal characteristics of the two compounds.

3.3. Electronic Properties. The calculated electronic band structures along the high symmetry directions in the Brillouin zones together with the total and site-projected l-decomposed DOS at equilibrium lattice parameters for $ACCr_3$ (A = Al and Ga) are shown in Figures 3 and 4. The band structures of the two compounds are very similar. Bands from −13 eV to −10 eV are mainly from the C-2s and Cr-3d states with strong hybridizations characteristic. From −8 eV to 2 eV, there are hybridizations between C-2p and Cr-3d states, and the Cr-3d states contribute dominantly to the bands, which suggests the itinerant nature of Cr-3d electrons. From Figure 4, it can be seen the Fermi level locates at the vicinity of the DOS peak, which leads large DOS at the Fermi level $N(E_F)$ with values of 4.79 states/eV for $AlCCr_3$ and 5.62 states/eV for $GaCCr_3$.

The Fermi surfaces of the two compounds are similar (see Figure 5). There are four bands that cross the Fermi level. Hole pockets surrounding Γ point come from the lower two bands (denoted with red and green colors in Figure 3). Electron pockets surrounding R point come from the upper two bands (denoted with blue and purple colors in Figure 3). The differences of the Fermi surface of the two compounds come from the band denoted with blue color in Figure 3. It crosses the Fermi level at the vicinity of M point for $AlCCr_3$, which makes the electron pockets surround the corners of the Brillouin zones connected to each other at M point. However, for $GaCCr_3$, it crosses the Fermi level in the place between Γ and M points, which forms a cubic cage-like electron pocket surrounding Γ point and connecting with the corner-centered electron pockets. The presence of electron and hole bands crossing the Fermi level indicates the multiple-band natures for $AlCCr_3$ and $GaCCr_3$.

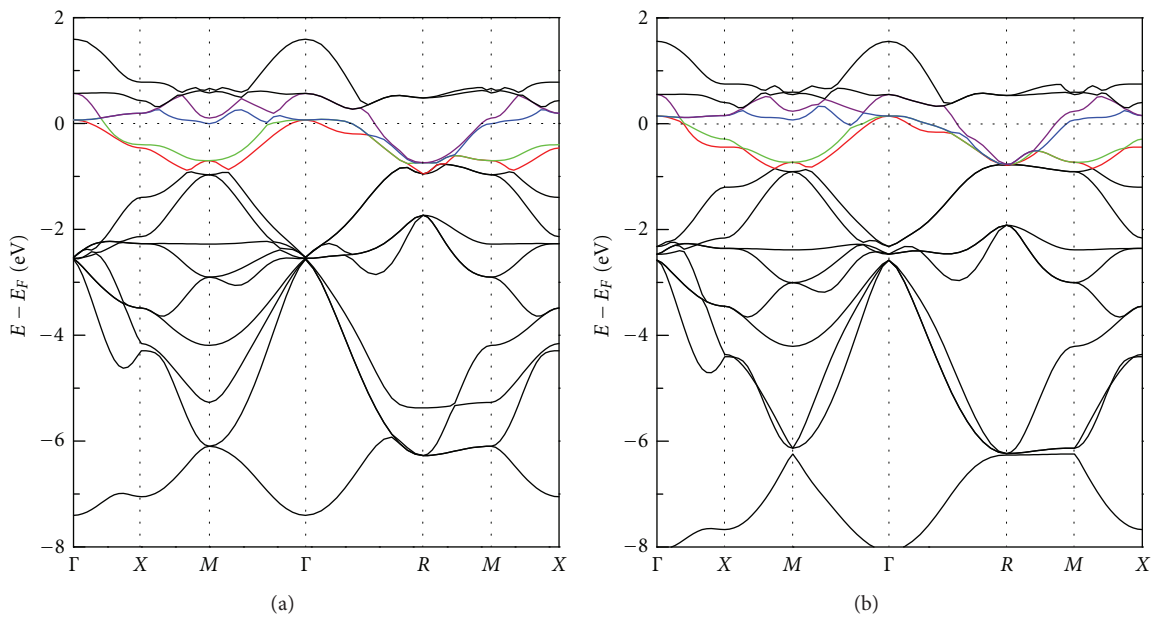

Figure 3: The band structures for (a) $AlCCr_3$ and (b) $GaCCr_3$. The colored lines denote the bands crossing the Fermi level.

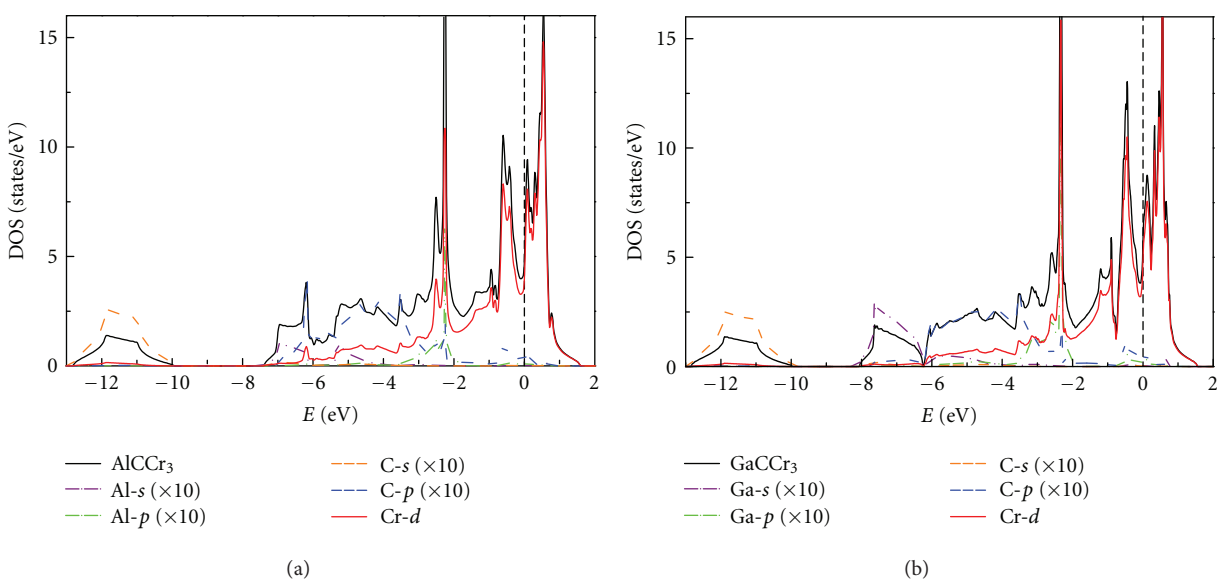

Figure 4: The density of states of (a) $AlCCr_3$ and (b) $GaCCr_3$.

In order to understand the bonding nature among the atoms in $AlCCr_3$ and $GaCCr_3$, we plot the contour maps of the charge density of the two compounds in Figure 6. The C–Cr bonds are very strong, which coincides with the strong hybridization between C-2p and Cr-3d electrons shown in DOS figures. The similarity of the bonding nature for the two compounds coincides with the similar Young's modulus E discussed before.

The electronic properties of $AlCCr_3$ and $GaCCr_3$ are very similar to those of the superconducting antiperovskite $MgCNi_3$ [37], for which the Fermi level locates at the vicinity of the DOS peak as well, and there is multiple-band nature present. The similarity possibly makes $AlCCr_3$ and $GaCCr_3$ potential superconductors. According to McMillan's coupling theory [38], the electron-phonon coupling constant λ can be calculated from the following expression $\lambda = \sum_\alpha(\eta_\alpha/M_\alpha\langle\omega_\alpha^2\rangle)$, where M_α is the atomic mass and $\langle\omega_\alpha^2\rangle$ is the averaged phonon frequency and can be approximated as $\langle\omega_\alpha^2\rangle = \Theta_D^2/2$. For superconducting $MgCNi_3$, there is a peak (a van Hove singularity) in DOS just below Fermi level, which leads to a large $N(E_F)$. The $N(E_F)$ is not large enough to lead magnetic instability, but it can lead to a large electron-phonon coupling constant [39]. To the best of our knowledge, except for the superconducting nickel antiperovskites, there are no

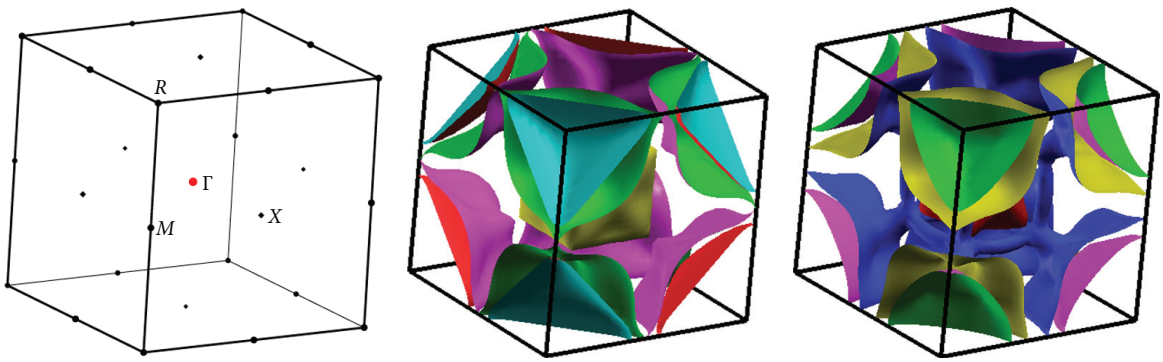

(a) (b) (c)

Figure 5: (a) Brillouin zone of $ACCr_3$. Fermi surfaces of (b) $AlCCr_3$ and (c) $GaCCr_3$.

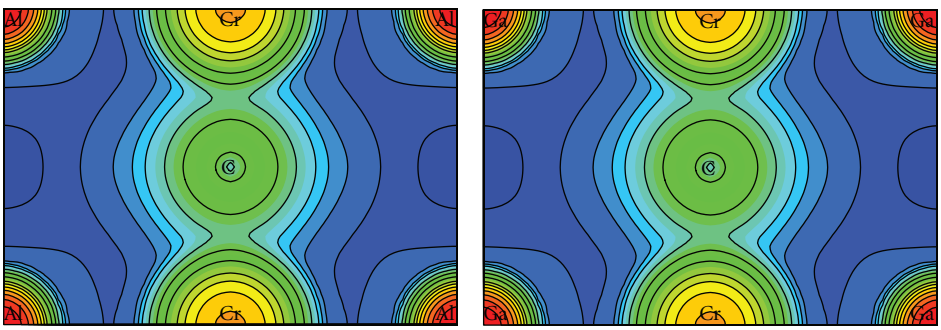

(a) (b)

Figure 6: The contour map of electron charge density of (a) $AlCCr_3$ and (b) $GaCCr_3$.

other antiperovskites that have such a nature. Wiendlocha et al. [17] pointed out that in chromium systems, chromium atoms have very large values of the McMillan-Hopfield parameters [38], which may lead to a very strong electron-phonon coupling. The recently reported work about $RhNCr_3$ [18] supports Wiendlocha et al.'s prediction. The phonon and electron-phonon coupling calculations show that $RhNCr_3$, which has a large $N(E_F)$, is a strong coupling superconductor with Tc above 16 K. Therefore, we consider that there is possibility for superconductivity appearing in $AlCCr_3$ and $GaCCr_3$. Phonon and electron-phonon coupling calculations will be carried out in the future to confirm the possibility.

4. Conclusion

In conclusion, we theoretically investigated the antiperovskite chromium-based carbides $ACCr_3$ through the first-principles calculation based on density functional theory. The optimized lattice parameter of $ACCr_3$ is basically proportional to the radius of A-site elements. Only $AlCCr_3$ and $GaCCr_3$ have negative formation energies, implying that the two compounds can be synthesized at ambient pressure and are stable with nonmagnetic ground states. $AlCCr_3$ and $GaCCr_3$ show ductile natures, and they may have similar thermal properties. Similar to superconducting antiperovskite $MgCNi_3$, there are electron and hole bands that cross the Fermi level for $AlCCr_3$ and $GaCCr_3$, indicating multiple-band natures. The Fermi level locates at the vicinity of the DOS peak, which leads to a large $N(E_F)$ dominated by Cr-3d electrons. These similarities possibly make $AlCCr_3$ and $GaCCr_3$ show superconductivity, which needs to be further investigated from theoretical and experimental studies.

Acknowledgments

This work was supported by the National Key Basic Research under Contract no. 2011CBA00111 and the National Nature Science Foundation of China under Contract nos. 91222109, 11274311, 51171177, 11174295, U1232139, and 50701042. The calculations were partially performed at the Center for Computational Science, CASHIPS.

References

[1] T. He, Q. Huang, A. P. Ramirez et al., "Superconductivity in the non-oxide perovskite $MgCNi_3$," *Nature*, vol. 411, no. 6833, pp. 54–56, 2001.

[2] M. Uehara, T. Yamazaki, T. Kôri, T. Kashida, Y. Kimishima, and I. Hase, "Superconducting properties of $CdCNi_3$," *Journal of the Physical Society of Japan*, vol. 76, no. 3, Article ID 034714, 2007.

[3] M. Uehara, A. Uehara, K. Kozawa, and Y. Kimishima, "New antiperovskite-type superconductor ZnN_yNi_3," *Journal of the Physical Society of Japan*, vol. 78, no. 3, 2009.

[4] K. Kamishima, T. Goto, H. Nakagawa et al., "Giant magnetoresistance in the intermetallic compound Mn_3GaC," *Physical Review B*, vol. 63, no. 2, Article ID 024426, 2001.

[5] Y. B. Li, W. F. Li, W. J. Feng, Y. Q. Zhang, and Z. D. Zhang, "Magnetic, transport and magnetotransport properties of $Mn_{3+x}Sn_{1-x}C$ and $Mn_3Zn_ySn_{1-y}C$ compounds," *Physical Review B*, vol. 72, no. 2, Article ID 024411, 2005.

[6] T. Tohei, H. Wada, and T. Kanomata, "Negative magnetocaloric effect at the antiferromagnetic to ferromagnetic transition of Mn_3GaC," *Journal of Applied Physics*, vol. 94, no. 3, pp. 1800–1802, 2003.

[7] M. H. Yu, L. H. Lewis, and A. R. Moodenbaugh, "Large magnetic entropy change in the metallic antiperovskite Mn_3GaC," *Journal of Applied Physics*, vol. 93, no. 12, pp. 10128–10130, 2003.

[8] K. Takenaka and H. Takagi, "Giant negative thermal expansion in Ge-doped anti-perovskite manganese nitrides," *Applied Physics Letters*, vol. 87, no. 26, Article ID 261902, pp. 1–3, 2005.

[9] K. Takenaka, K. Asano, M. Misawa, and H. Takagi, "Negative thermal expansion in Ge-free antiperovskite manganese nitrides: tin-doping effect," *Applied Physics Letters*, vol. 92, no. 1, Article ID 011927, 2008.

[10] K. Asano, K. Koyama, and K. Takenaka, "Magnetostriction in Mn_3 CuN," *Applied Physics Letters*, vol. 92, no. 16, Article ID 161909, 2008.

[11] E. O. Chi, W. S. Kim, and N. H. Hur, "Nearly zero temperature coefficient of resistivity in antiperovskite compound $CuNMn_3$," *Solid State Communications*, vol. 120, no. 7-8, pp. 307–310, 2001.

[12] J. C. Lin, B. S. Wang, P. Tong et al., "Tunable temperature coefficient of resistivity in C- and Co-doped $CuNMn_3$," *Scripta Materialia*, vol. 65, no. 5, pp. 452–455, 2011.

[13] B. T. Matthias, T. H. Geballe, V. B. Compton, E. Corenzwit, and G. W. Hull, "Superconductivity of chromium alloys," *Physical Review*, vol. 128, no. 2, pp. 588–590, 1962.

[14] Y. Nishihara, Y. Yamaguchi, T. Kohara, and M. Tokumoto, "Itinerant-electron antiferromagnetism and superconductivity in bcc Cr-Re alloys," *Physical Review B*, vol. 31, no. 9, pp. 5775–5781, 1985.

[15] Y. Nishihara, Y. Yamaguchi, M. Tokumoto, K. Takeda, and K. Fukamichi, "Superconductivity and magnetism of bcc Cr-Ru alloys," *Physical Review B*, vol. 34, no. 5, pp. 3446–3449, 1986.

[16] H. L. Alberts, D. S. McLachlan, T. Germishuyse, and M. Naidoo, "Superconductivity and antiferromagnetism in Cr-Mo-Ru alloys," *Journal of Physics*, vol. 3, no. 12, pp. 1793–1800, 1991.

[17] B. Wiendlocha, J. Tobola, S. Kaprzyk, and D. Fruchart, "Electronic structure, superconductivity and magnetism study of Cr_3GaN and Cr_3RhN," *Journal of Alloys and Compounds*, vol. 442, no. 1-2, pp. 289–291, 2007.

[18] H. M. Tütüncü and G. P. Srivastava, "Phonons and superconductivity in the cubic perovskite Cr_3RhN," *Journal of Applied Physics*, vol. 112, no. 9, Article ID 093914, 2012.

[19] P. E. Blöchl, "Projector augmented-wave method," *Physical Review B*, vol. 50, no. 24, pp. 17953–17979, 1994.

[20] M. Torrent, F. Jollet, F. Bottin, G. Zérah, and X. Gonze, "Implementation of the projector augmented-wave method in the ABINIT code: application to the study of iron under pressure," *Computational Materials Science*, vol. 42, no. 2, pp. 337–351, 2008.

[21] X. Gonze, J. M. Beuken, R. Caracas et al., "First-principles computation of material properties: the ABINIT software project," *Computational Materials Science*, vol. 25, no. 3, pp. 478–492, 2002.

[22] X. Gonze, B. Amadon, P. M. Anglade et al., "ABINIT: first-principles approach to material and nanosystem properties," *Computer Physics Communications*, vol. 180, no. 12, pp. 2582–2615, 2009.

[23] X. Gonze, G. M. Rignanese, M. Verstraete et al., "A brief introduction to the ABINIT software package," *Zeitschrift fur Kristallographie*, vol. 220, no. 5-6, pp. 558–562, 2005.

[24] J. P. Perdew, K. Burke, and M. Ernzerhof, "Generalized gradient approximation made simple," *Physical Review Letters*, vol. 77, no. 18, pp. 3865–3868, 1996.

[25] H. J. Monkhorst and J. D. Pack, "Special points for Brillouin-zone integrations," *Physical Review B*, vol. 13, no. 12, pp. 5188–5192, 1976.

[26] F. Birch, "Finite elastic strain of cubic crystals," *Physical Review*, vol. 71, no. 11, pp. 809–824, 1947.

[27] F. D. Murnaghan, *Finite Deformation of An Elastic Solid*, Dover Publications, New York, NY, USA, 1951.

[28] J. Zhao, J. M. Winey, and Y. M. Gupta, "First-principles calculations of second- and third-order elastic constants for single crystals of arbitrary symmetry," *Physical Review B*, vol. 75, no. 9, Article ID 094105, 2007.

[29] R. Hill, "The elastic behaviour of a crystalline aggregate," *Proceedings of the Physical Society A*, vol. 65, no. 5, pp. 349–354, 1952.

[30] D. C. Wallace, *Thermodynamics of Crystals*, John Wiley & Sons, New York, NY, USA, 1972.

[31] D. J. Green, *An Introduction to the Mechanical Properties of Ceramics*, Cambridge University Press, Cambridge, UK, 1998.

[32] R. E. Newnham, *Properties of Materials; Anisotropy, Symmetry, Structure*, Oxford University Press, New York, NY, USA, 2005.

[33] D. G. Pettifor, "Theoretical predictions of structure and related properties of intermetallics," *Materials Science and Technology*, vol. 8, no. 4, pp. 345–349, 1992.

[34] S. Pugh, "Relations between the elastic moduli and the plastic properties of polycrystalline pure metals," *Philosophical Magazine Series*, vol. 7, no. 45, pp. 823–843, 1954.

[35] J. Haines, J. M. Léger, and G. Bocquillon, "Synthesis and design of superhard materials," *Annual Review of Materials Research*, vol. 31, pp. 1–23, 2001.

[36] V. Kanchana, "Mechanical properties of Ti_3AlX (X = C, N): Ab initio study," *Europhysics Letters*, vol. 87, no. 2, p. 26006, 2009.

[37] S. Mollah, "The physics of the non-oxide perovskite superconductor $MgCNi_3$," *Journal of Physics Condensed Matter*, vol. 16, no. 43, pp. R1237–R1276, 2004.

[38] W. L. McMillan, "Transition temperature of strong-coupled superconductors," *Physical Review*, vol. 167, no. 2, pp. 331–344, 1968.

[39] J. H. Shim, S. K. Kwon, and B. I. Min, "Electronic structures of antiperovskite superconductors $MgXNi_3$ (X = B, C, and N)," *Physical Review B*, vol. 64, no. 18, Article ID 180510, 2001.